Journal of Physics:
Conference Series

PAPER • **OPEN ACCESS**

Optical analysis of the deposition and detachment phenomena experienced by an airfoil leading edge

To cite this article: Nicola Zanini *et al* 2025 *J. Phys.: Conf. Ser.* **3063** 012010

Journal of Physics: Conference Series **3063** (2025) 012010 doi:10.1088/1742-6596/3063/1/012010

Optical analysis of the deposition and detachment phenomena experienced by an airfoil leading edge

Nicola Zanini* , **Alessio Suman** , **Francesco Bosi, Mattia Piovan** , **Michele Pinelli**

Department of Engineering - University of Ferrara, Via Saragat 1, 44122, Ferrara, Italy

E-mail: nicola.zanini@unife.it

Abstract. Solid micro-particle ingestion is one of the principal degradation mechanisms in compressor sections. In industrial applications, micro-particles not captured by the air filtration system cause fouling and, consequently, a performance drop. Even if, in the last decade, manufacturers have been oriented to the development of transonic axial compressors, subsonic stages are commonly used for heavy-duty industrial applications such as pump stations and process compressors thanks to their very high reliability and relatively restrained cost (maintenance and recovery). This works presents an analysis of the deposition and detachment phenomena experienced by an airfoil leading edge. The experimental tests are carried out using micro-particles and two flow velocities. A non-contact continuous measurement process has been realized to discover the over-the-time modification of the deposit build-up and detachment that characterized the leading edge region. The measuring process is based on the image capture of the blade surface, comparing two subsequent frames, and recognizing the light intensity variation. Using such a strategy, this method generates a history of modifying the light intensity pixel by pixel. A recursive process has been highlighted after an initial phase representing the evolution of the surface condition from clean to fouled operating condition. Guidelines for interpreting the fouling behavior of a blade profile are proposed.

1. Introduction

Air pollutants can greatly impact the overtime performance of many industrial devices [1], which usually drops depending on the contamination severity. The local atmospheric contamination is generally constituted by particles coming from different sources (natural or anthropogenic) with different chemical and size, making the determination of the real aerosols' composition very challenging [2, 3]. Although in the recent decades remote sensing techniques [4, 5] improved the prediction quality and reliability of environmental aerosols measurements, the effects that such contamination generates on the industrial devices are still not fully understood.

Gas turbines are commonly employed worldwide for power generation and in gas compression stations, even in harsh contaminated environments. Here, multi-stage filtration systems are installed to reduce the amount of the incoming contaminants [6, 7], preserving the life of the machine. Anyway, the finer particles fraction (< 1 μm) could escape the filter barrier reaching the compressor unit [8]. Depending on the particles' type, size, and dynamic conditions, the interaction with the internal surfaces of the machine may lead to deposition or, in the worst cases, even to corrosion and erosion phenomena [9]. In the first case, the progressive adhesion of particles involves the formation of deposited layers which alters the blades' shape and roughness

resulting in aerodynamic losses [10, 11, 12]. Such phenomenon is also known as fouling, and it is classified a recoverable degradation phenomenon with cleaning/washing operations. Erosion and corrosion instead, can severely compromise the safety of operations and require major overhaul with the replacement of damaged components.

Usually, the fouling severity is monitored indirectly by evaluating the compressor performance parameters, e.g. efficiency, mass flow rate and pressure ratio variation with the exposure time [12]. Some attempts to define fouling susceptibility factors can be found in literature [13, 14] which predict the compressor performance variation without modeling the deposition behavior. On-field experiences have shown that fouling tends to occur during initial operation and roughly follows an exponential law, stabilizing after 1000 hours of operations [13]. However, no information regarding deposits over time is found as the machines are only inspected during major overhauls. Kurz et al. [15] carried out deposition test in a wind tunnel on a stationary blade obtaining that the particle distribution on a dry airfoil can be accurately predicted using different models from the literature, while with wet (i.e. humid) blades the predictions fall. Particles sticking is greatly influenced by the wetness of the airfoil and thus, the relative humidity of the incoming air plays a fundamental role in the adhesion process [16]. The influence of relative humidity in particles deposition was also tested in an axial compressor test rig [17, 18]. In [17], the effects of compressor fouling are investigated in an environment with controlled levels of contamination and relative humidity obtaining that the compressor performance decreasing more rapidly in humid conditions. In [18] the blades leading edge of the IGV and the first rotor stage were analyzed after the exposure to soil contaminants obtaining clearly distinguishable results depending on the relative humidity: for high humid air, the deposit appears compact and uniform along the span; in dry condition instead, the shape of the deposit appears fragmented and discontinuous. The magnitude of the detachments detected appears again proportional to humidity: high relative humidity involves larger and less frequent detachments. Lab-scale experimental investigations on particles deposition highlighted how the development of the deposit on a clean flat target follows a logistic trend [19]: a first monotonous growth is followed by a cyclical fluctuation of the deposited mass due to the succession of detachment and re-deposition phenomena. Although the model in [19] is able to reliably predict the time fouling behavior on a simplified target, it is not possible to establish whether this can be extended to real machine geometries since there is no information in the open literature about the continuous evolution of deposition on compressor blades.

This work proposes a measuring procedure based on image analysis techniques to monitor the overtime fouling behavior on a stationary cascade in a wind tunnel. A video acquisition system coupled with a decision-making algorithm allows to evaluate the progressive degree of fouling on the cascade and establish when detachments occur. The timing of occurrence and size of the detachments open to future modeling of the phenomenon and thus, the performance prediction of the machine.

2. Test Rig

The fouling behavior overtime is evaluated performing deposition test in the wind tunnel located at the Unife Labs [20] which was specifically to reproduce first stages compressor-like conditions (i.e., impact velocity, relative humidity, and temperature). The wind tunnel here considered is an open-loop that provides the necessary airflow to perform particle deposition tests on a stationary cascade. An overview of the test rig is shown in Fig. 1.

The rig works by taking air from the outside and it mainly consists of two sections: (i) the conditioning section and (ii) the pneumatic transport section. The airflow is provided by a 30 kW blower which reaches a total pressure of 25,000 Pa. The air first enters the conditioning section where it passes through an air handling unit (AHU) and reaches the desired thermo-hygrometric conditions. The relevant measuring points for relative humidity and temperature

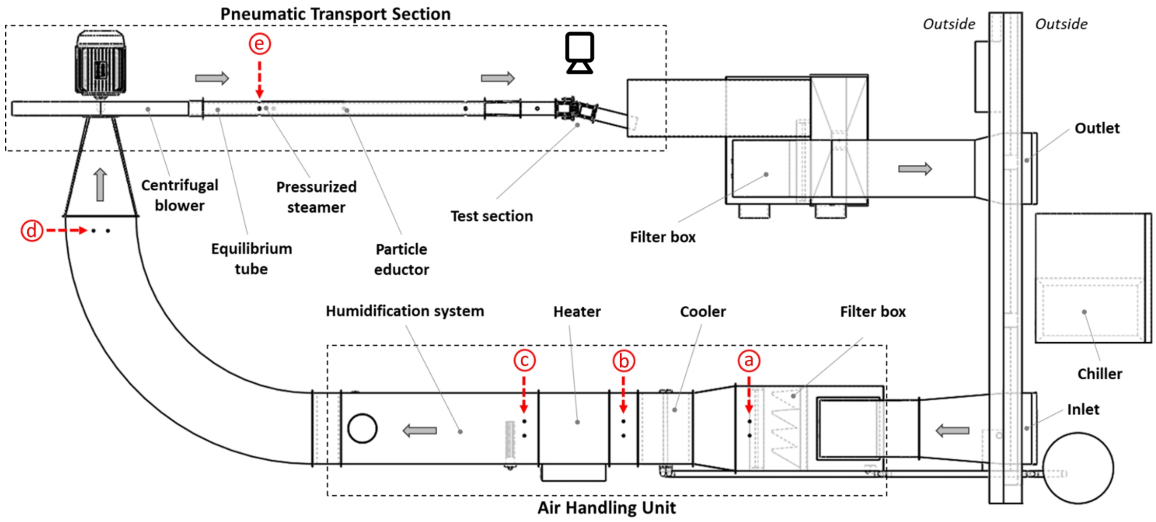

Figure 1: Wind Tunnel [20]

have been marked with letters from a to e in Fig.1. Downstream of the AHU, the air accelerates in the pneumatic transport section, and a precise amount of dust is injected. The aerosol enters the equilibrium tube (see Fig.1), where a pressurized steamer can adjust the relative humidity since the centrifugal blower increases the airflow temperature from the control point d to e. Afterward, the air reaches the test section where the stationary cascade is located and the residual contaminants are removed from the exhaust airflow with media filters before blowing out the air. The feeding unit is a Solid Aerosol Generator SAG 410/Ultralowflow made by TOPAS® GmbH. This device provides the correct dosage of the powder mass constantly with high instantaneous precision of the metering process and, at the same, it is suitable for continuous feeding process [21, 22]. A rotating ring is charged with the powder in a drizzling manner employing a conveyor system, and the powder is carried at a constant speed from the charging site to the sucking dispersing nozzle. This dispersing nozzle allows the first deagglomeration and dispersion of the powder. After the sucking zone, to ensure the repeatability of the dosing process, the ring is continuously cleaned by a brush that removes the residual (if present) particles on the rotating ring. For more details regarding the feeding process and the test rig, the reader is referred respectively to [22] and [20].

The test section consists in a 50 x 50 mm rectangular duct. The target is a 5-blades stationary cascade, whose schematic view is shown in Fig. 2a. As reported in the literature [23], a minimum number of five blades is recommended to reduce the effects of boundary conditions. In the present design, the cascade comprises five blades to achieve suitable flow periodicity. The central blades are thus considered for the measurements (A, B, C in Fig.2a), while adjacent blades are inserted to obtain a uniform flow field. Two optical accesses (before and after the cascade) are provided for the bottom side and the side walls of the test section, while the top wall has a removable cover from which the three central blades can be removed. The blades feature NACA 7418 airfoils and the design parameters are shown in Fig. 2b, while the airfoil height equals 50 mm. The reference free-stream air velocity in front of the cascade is equal to 86.7 m/s.

The overtime deposition history is recorded using an HD camera that overlooks the cascade from one optical access on the sidewall with focus on the three central blades. The positioning of the camera relative to the test section and a representative frame of the cascade is shown in Fig. 3. Videos are acquired during the deposition test with a frame rate of 10 fps and the resolution is 1600x1200 ppi, resulting in a scale 20.96 pixel/mm.

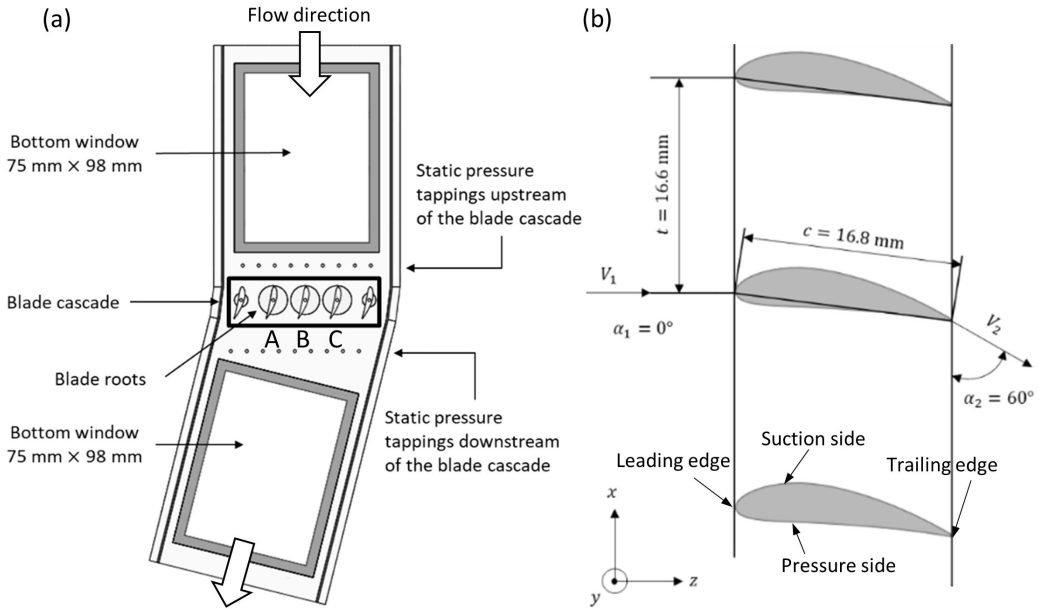

Figure 2: Test section - (a) Layout; (b) Blade Profile

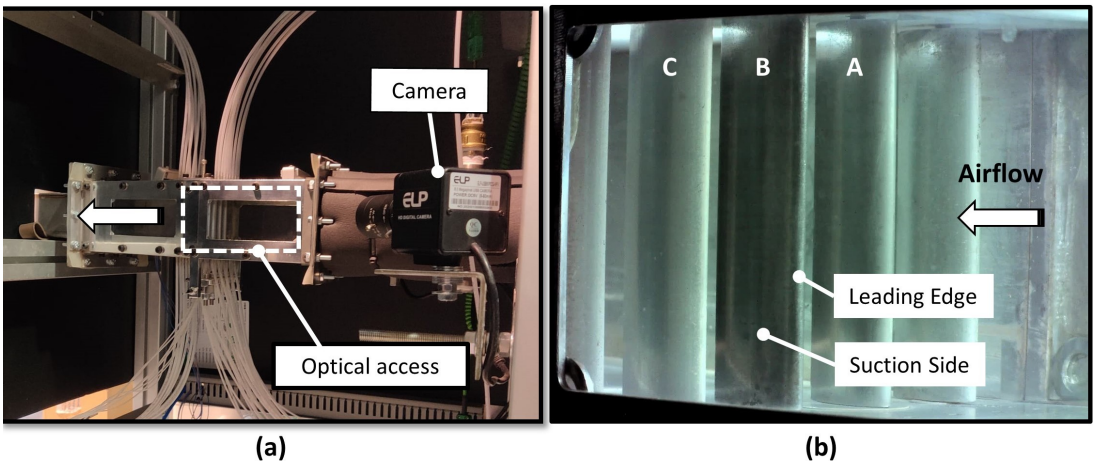

Figure 3: Video acquisition setup (a) Test rig layout; (b) Camera framing

3. Fouling Detection Tool

The overtime fouling behavior for a stationary target in the wind tunnel is analyzed employing an in-house routine implemented in MATLAB®. Basing on the videos acquired during the deposition test, the tool aims to detect the progressive particles stacking and sudden deposit detachment that may occur when the dust load limit for a surface is reached.

3.1. Pre-Process and Calibration

The acquired time-lapse videos of the deposition test are post processed using an in-house MATLAB routine to get the time occurrence and size of the detachments. Time-lapse videos are loaded into MATLAB through the *VideoReader* function, which extracts all the frames as true-color RGB image. Each frame is stored into a (n x m x 3) matrix, where n and m are image size in pixels, while the third dimension corresponds to the RGB level of the single pixel. Matrices obtained processing all the frames are then collected in a cell structure.

Deposit detachments are sudden events of material loss from the substrate that may cause a clear change in light intensity in true-color RGB images where the detachment occurs [19]. Depending on the operating conditions (relative humidity and temperature), the detachment could even leave the surface of the substrate completely clean [18]. Taking advantage of this characteristic, detachments can be detected comparing two consecutive frames and observing the change in light intensity. Modern descriptor-based image recognition systems employ grayscale since it usually simplifies the algorithm and reduces computational requirements [24]. Indeed, colors may introduce unnecessary information increasing the amount of training data required to achieve good performance. RGB images are here converted into grayscale images using the *rgb2gray* function, which calculates the grayscale value according to Eq.1.

$$I = 0.299 \cdot R + 0.587 \cdot G + 0.114 \cdot B \tag{1}$$

Where R, G and B refer respectively to red, green and blue values. The function converts RGB data into a single greyscale value between 0 (black) to 255 (white), thus reducing the size of each frame matrix. Single or multiple user-defined regions of interest (ROI) can be defined according to the needs to reduce the size of the investigation area and therefore the computational effort. Since the optical properties of particulate and substrate materials determine the light absorption and scattering, a calibration procedure is required to determine how the light intensity (greyscale representation) of the target changes while deposition and detachment phenomena occur. Preliminary deposition test is performed to observe the effect of a deposited layer onto the target surface. Visual inspection combined with the analysis of the greyscale frames allows for the determination of the light variation trend. Additionally, a user-defined threshold value α can be defined, which allows filtering out background noise due to fouling of the inspection window glass. Such parameter should be set according to the concentration of the particles considered during the test and it can be derived comparing two subsequent frames without detachment.

3.2. Process

The fouling behavior is obtained by observing the light variation of corresponding pixels internal to the ROI between two consecutive frames, i.e. for the instants t and $t + \Delta t$ where Δt can be varied according to the video frame rate. Each frame of the ROI is represented by a (n x m) matrix corresponding to the number of pixels in horizontal and vertical direction respectively, as a sketch in Fig. 4.

The grayscale intensity variation ΔI, which is calculated as the absolute value of the difference between the grayscale intensity of the frame at t and $t + \Delta t$, is considered to establish the

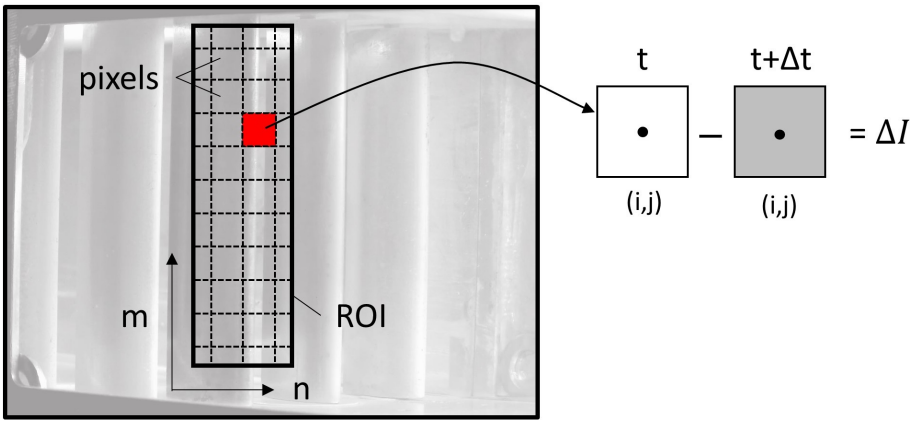

Figure 4: Conceptualization of pixel analysis over time

occurrence of deposition and/or detachment phenomena. As reported in Sec. 1, the time of occurrence of deposition and detachment can be very different: while the effects of deposition are clearly visible after minutes or hours of exposure time to contaminants, detachments occur suddenly with characteristic times of seconds or less. Consequently, different time steps (Δt) should be considered to appreciate the deposition or sample occurrence times and sizes of detachments over time. The methodology presented can be employed for both the aims but here it mainly focuses on the detachments analysis since it requires a faster response time and to process a greater number of frames compared to the fouling analysis.
The value of I of the single pixel in position (i,j) at time t is extracted from the frame matrix and subtract to the following time step, obtaining ΔI. Such parameter is then compared with a user-defined threshold value ϵ, which allows to determine the detachment condition of the single pixel. The procedure is then repeated for all pixels contained in the ROI and the position of the pixels are stored only if the detachment condition is satisfied. As described in Sec. 3.1, the parameter α is employed to filter the fouling of the inspection window and for the actual cascade it is estimated between 2 and 3 of the grayscale units.
In order to filter possible false positives, a decision algorithm is defined to determine whether a detachment has occurred on the target based on the topological distribution of the individual "detached" pixels. Real deposits detachments are defined when a minimum number of neighboring-filtered pixels N_{min} are found in a specified control area A, whose dimensions (w, z) can be freely set by the user. Two pixels are considered neighbors if they share at least one vertex of the ROI grid (Fig.4. Starting from the top left corner of the frame, the centroid of the control area is moved one pixel at a time along the row, and the routine sums all the detached pixels (N_{det}) within the control area at each step. When the condition $N > N_{min}$ is satisfied, all the detached pixels (N_{det}) constitute a single detachment entity, whose size is equal to the area of the detached pixels. Once the row is analyzed, the next one is considered iterating the loop. A depiction of the controlled area within the ROI is reported in Fig. 5.
Once the ROI is analyzed, the routine calculates the resulting detached areas for all the times steps recording the size and the times of occurrence of deposits removal.

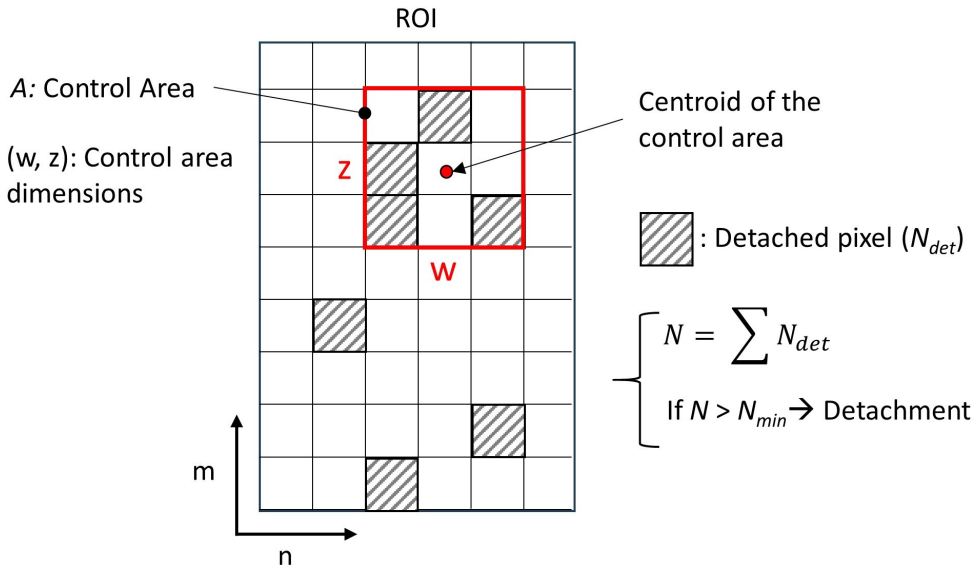

Figure 5: Sketch of the control area within the ROI

3.3. Results and Statistics

At the end of the analysis, deposits and detachments statistics are computed and for each frame and for the entire duration of the test. Detachments are evaluated in terms of percentage of ROI area, times of occurrence and localization within the ROI. Average size and relative standard deviation are computed as well to highlight where detachments occur more frequently and/or with greater size. According to [19, 10], detachment phenomena are induced by shear stresses acting on the target surface that overcome the adhesion forces (e.g. capillarity, Van der Waals). Depending on the flow conditions, the topological evaluation of the detachments allows to qualitatively estimate where the greatest aerodynamic stresses develop on the target. Additionally, the results are graphically proposed by superimposing the areas subject to detachment to the original frame.

4. Test Case

The validity of the methodology is tested carrying out deposition test on a stationary cascade in a wind tunnel. Two blades featuring NACA 7418 airfoils with different substrate color are considered for the deposition test, i.e. black (Blade A), and grey (Blade B), as reported in Fig. 6. Since most of the deposits are usually detected on the blade's leading edge, a region of interest (ROI) is defined at the leading edge of each blade to carry out the analysis of the detachment behavior overtime (see Fig. 6a). Preliminary deposition test confirmed the stacking of particles along the blade leading edge, as shown in Fig. 6b, where detachments are marked in red.

Deposition test is performed at the design free-stream air velocity for the cascade, i.e. 86.7 m/s, for four hours with 50 %RH. The selected contaminant is Arizona Road Dust (ARD), which is a standardized powder commonly employed for filter evaluation [25]. ARD is representative of the contamination coming from natural sources (e.g. soil) and it mainly consisting of about 70 wt.% silica and 14 wt.% aluminum oxide and other minor [26]. The average particle diameter for the selected grade of ARD here considered is 1.3 μm and the test are carried in constant concentration condition equals to 6.12 mg/m^3. Preliminary numerical analysis [20] proved that the length of the equilibrium tube is sufficient to reach the thermal and dynamic equilibrium of the ARD powder with the flow conditions here considered. The functionality of the fouling

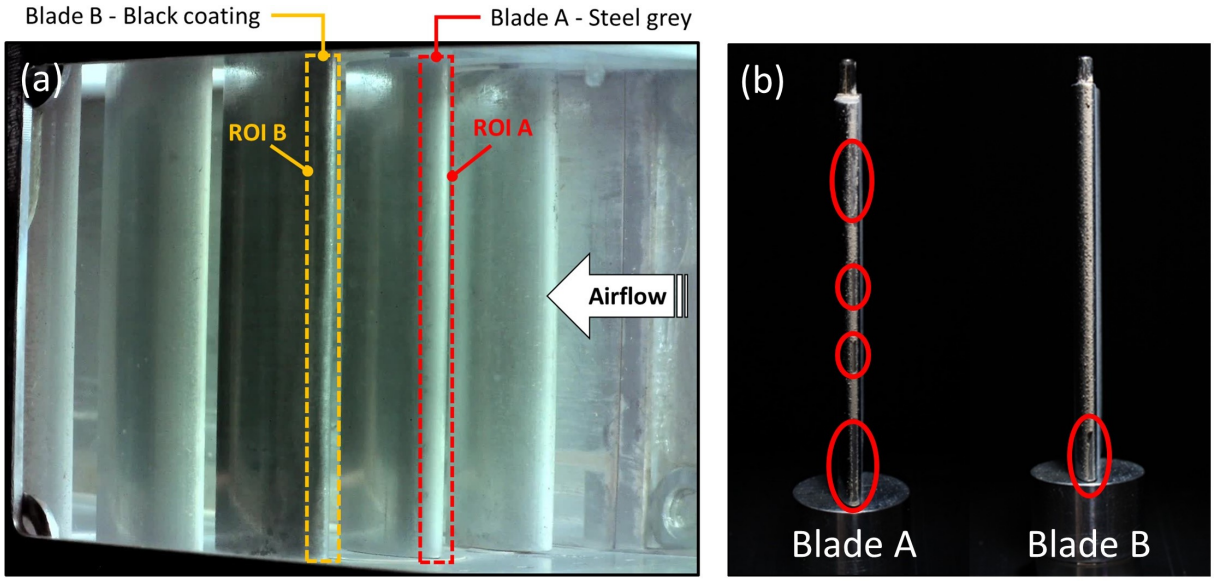

Figure 6: Test case - (a) ROI of the steel grey (blade A) and black (blade B) airfoils; (b) Detachment over the blade leading edge

analysis tool is tested by looking for detachments after three hours of exposure to contaminants. The main steps of the process are summarized in Fig. 7. First, the subtraction of two consecutive greyscale frames allows the detection of detached pixels (Fig.7 a, b). Then, the topological filter removes the pixels classified as false positive obtaining the real detachment occurred on the blade leading edge (Fig.7 c, d). For the actual test case, the threshold for the definition of a detached pixel ϵ was set equal to 5, while the minimum number of pixel in the control area N_{min} was imposed equal to 10. Visual inspection confirms the presence of a remarkable detachment on the bottom part of the blade for the frame considered.

Following the same strategy, a trial run of the tool is executed to investigate the onset of detachments on blade A (steel grey) for 18.5 seconds after an exposure time of three hours. The resulting statistics expressed as a percentage of the ROI A are reported in Fig. 8. Detachments

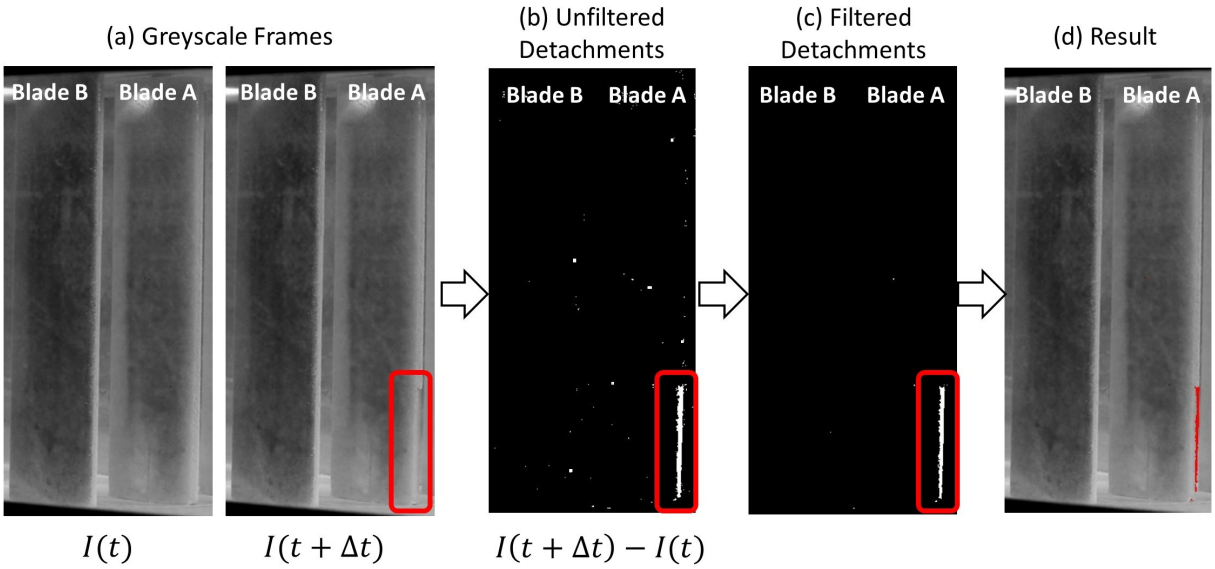

Figure 7: Image post processing for a trial run of the tool

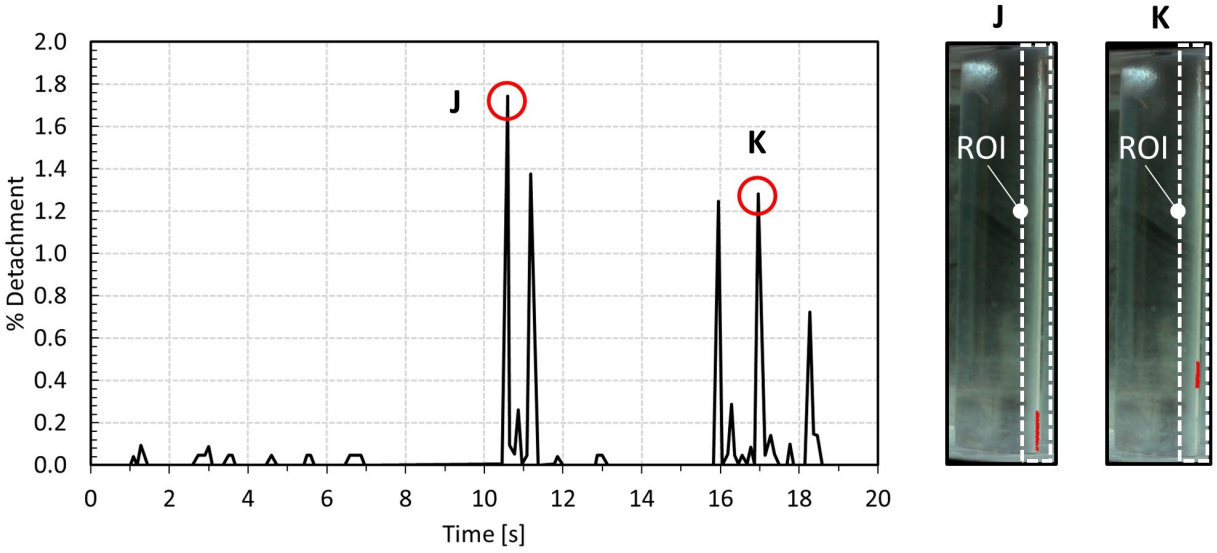

Figure 8: Detachment detection after three hours of exposure time for 18.5 seconds

are detected throughout the blade leading edge reaching a maximum of 1.8 % and an average of 0.25 % of the ROI. Additionally, few examples of detachments superimposed on the true color RGB frames (J, K) are reported in Fig. 8.

5. Conclusions and Remarks

This contribution aims to present a non-intrusive image-based technique to monitor the fouling behavior overtime on a target surface. A MATLAB routine is defined to analyze the evolution of deposition on the relevant surfaces (e.g. leading edge) of aerodynamic profiles including detachment phenomena. The feasibility of the fouling behavior detection overtime through image analysis techniques was tested in stationary cascade in a wind tunnel. Detachment detection was performed after three hours of exposure time to contaminants obtaining promising results for the online detection and surveillance of fouling severity. Further works will be devoted to test the methodology with different contaminants and on rotating machines (compressors, turbines, etc. . .). Fouling detections could also be correlated to the blade/cascade performance, e.g. lift, to define a prediction model only based on visual inspection.

References

[1] Kukulka D J, Czechowski H and Kukulka P D 2010 *Heat Transfer Engineering* **31** 782 – 787
[2] Pöschl U 2005 *Angewandte Chemie - International Edition* **44** 7520 – 7540
[3] Ault A P and Axson J L 2017 *Analytical Chemistry* **89** 430 – 452
[4] Ansmann A and Müller D 2005 Lidar and atmospheric aerosol particles *Lidar* (Springer) pp 105–141
[5] Omar A H, Winker D M, Vaughan M A, Hu Y, Trepte C R, Ferrare R A, Lee K P, Hostetler C A, Kittaka C, Rogers R R *et al.* 2009 *Journal of Atmospheric and Oceanic Technology* **26** 1994–2014
[6] Wilcox M 2011 *Mechanical Engineering* **133** 48 – 49
[7] Perullo C A, Lieuwen T, Barron J, Grace D and Angello L 2015 Evaluation of air filtration options for an industrial gas turbine vol 3
[8] Kurz R and Brun K 2012 *Journal of Engineering for Gas Turbines and Power* **134**
[9] Suman A, Morini M, Aldi N, Casari N, Pinelli M and Spina P R 2017 *Journal of Turbomachinery* **139** 041005
[10] Friso R, Suman A, Vulpio A, Zanini N, Casari N and Pinelli M 2023 *International Journal of Heat and Mass Transfer* **200**
[11] Suder K, Chima R, Strazisar A and Roberts W 1995 *Journal of Turbomachinery* **117** 491 – 505
[12] Meher-Homji C B, Chaker M and Bromley A F 2009 The fouling of axial flow compressors - causes, effects, susceptibility and sensitivity vol 4 p 571 – 590
[13] Tarabrin A, Schurovsky V, Bodrov A and Stalder J P 1998 *Journal of Turbomachinery* **120** 256 – 261
[14] Seddigh F and Saravanamuttoo H 1991 *Journal of Engineering for Gas Turbines and Power* **113** 595 – 601
[15] Kurz R, Musgrove G and Brun K 2017 *Journal of Engineering for Gas Turbines and Power* **139** cited by: 35 URL `https://www.scopus.com/inward/record.uri?eid=2-s2.0-84992366163&doi=10.1115%2f1.4034501&partnerID=40&md5=9a8a28c1166bf6ea151971632263fcdc`
[16] Aldi N, Casari N, Dainese D, Morini M, Pinelli M, Spina P R and Suman A 2017 The effects of third substances at the particle/surface interface in compressor fouling vol 9
[17] Vulpio A, Suman A, Casari N, Pinelli M, Kurz R and Brun K 2021 *Journal of Engineering for Gas Turbines and Power* **143**
[18] Suman A, Zanini N and Pinelli M 2024 *Journal of Turbomachinery* **146**
[19] Suman A, Vulpio A, Casari N and Pinelli M 2021 *Powder Technology* **394** 597 – 607
[20] Suman A, Zanini N and Pinelli M 2023 Design of an innovative experimental rig for the study of deposition phenomena in axial compressors *Turbo Expo: Power for Land, Sea, and Air* vol 87103 (American Society of Mechanical Engineers) p V13CT31A009
[21] Casari N, Fortini A, Pinelli M, Suman A, Vulpio A and Zanini N 2022 *Measurement* **187** 110185 ISSN 0263-2241
[22] Suman A, Zanini N, Vulpio A and Pinelli M 2024 *Experimental Thermal and Fluid Science* **151** 111074 ISSN 0894-1777
[23] Hirsch C 1993 *NASA STI/Recon Technical Report N* **94** 15119
[24] Kanan C and Cottrell G W 2012 *PloS one* **7** e29740
[25] ISO 2024 *ISO 12103-1:2024*
[26] Vlasenko A, Sjögren S, Weingartner E, Gäggeler H and Ammann M 2005 *Aerosol Science and Technology* **39**

452 – 460 cited by: 83 URL https://www.scopus.com/inward/record.uri?eid=2-s2.0-20044372558&doi=10.1080%2f027868290959870&partnerID=40&md5=a506b8abb2149164a534488874207961